Int. J. Electrochem. Sci., 10 **(2015)** 3973 - 3987

International Journal of
ELECTROCHEMICAL
SCIENCE
www.electrochemsci.org

Formation of G-quadruplex and Its Utilizing for an Automated Spectrometric Detection of Cisplatin

Branislav Ruttkay-Nedecky[1,2], *Sylvie Skalickova*[1,2], *Monika Kremplova*[1,2], *Lukas Nejdl*[1,2], *Jiri Kudr*[1,2], *David Hynek*[1,2], *Marie Novotna*[1,2], *Jan Labuda*[3], *Vojtech Adam*[1,2] *and Rene Kizek*[1,2*]

[1]Department of Chemistry and Biochemistry, Mendel University in Brno, Zemedelska 1, CZ-613 00 Brno, Czech Republic
[2]Central European Institute of Technology, Brno University of Technology, Technicka 3058/10, CZ-616 00 Brno, Czech Republic
[3]Institute of Analytical Chemistry, Faculty of Chemical and Food Technology, Slovak University of Technology in Bratislava, Radlinskeho 9, 812 37 Bratislava, Slovak Republic
[*]E-mail: kizek@sci.muni.cz

Received: 12 January 2015 / *Accepted:* 24 February 2015 / *Published:* 23 March 2015

Here, we studied the formation of G-quadruplex using spectrophotometric methods (peroxidase activity of G-quadruplex) and verifications of obtained results by voltammetry (cytosine-adenine (CA) or guanine (G) peaks height). The results showed that the peroxidase activity of G-quadruplex increases with the increasing concentrations of K^+ ions (1-20 mM) and Na^+ ions (1-5 mM) with the highest values observed in the presence of K^+ ions. The reverse trend was obtained with NH_4^+ ions, where the highest peroxidase activity was observed at the lowest concentration of NH_4^+ ions. The G-quadruplex formation was also proven electrochemically. The addition of 5 mM of K^+ ions to the oligonucleotide solution with hemin caused a decrease of both determined peaks. The peroxidase activity of G-quadruplex increased with the increasing concentration of Ag^+ ions within the range from 40 nM to 5 μM. Further, the addition of different concentration of cisplatin (0.5-2 μM) to the G-quadruplex was monitored. With the addition of cisplatin there was a decrease in peroxidase activity and simultaneously decrease in the CA peak height with the greatest effect in twentieth minute after the addition of cisplatin. The G-quadruplex coupling with gold magnetic nanoparticles was performed and the possibility of automation of spectrophotometric assay was proven

Keywords: *G*-quadruplex; Silver Ions; Cisplatin; Spectrophotometric Methods; Square Wave Voltammetry; Cyclic Voltammetry

1. INTRODUCTION

Metalloporphyrins are the active cofactors for a wide variety of enzymes and specialized cellular proteins. Heme [Fe(II)-protoporphyrin IX] is a cofactor used by proteins such as hemoglobin

and myoglobin for reversible dioxygen binding. Hemin [Fe(III)-protoporphyrin IX] is a cofactor for a number of enzymes such as catalases, which degrade hydrogen peroxide, and peroxidases and monooxygenases, which also includes cytochrome P450 family [1,2]. In addition, hemin itself is capable to catalyze peroxidation reactions [3], although at much lower levels than those of hemin in enzymes such as horseradish peroxidase [4].

Guanine-rich sequences of DNA are able to create tetrastranded structures known as G-quadruplexes. These are formed by the stacking of planar G-quartets composed of four guanines paired by Hoogsteen hydrogen bonding [5]. G-quadruplexes are also stabilized by the presence of alkali metal ions (Na^+ or K^+), which are located in the center between two G-quartets [6]. Interestingly, G-quadruplexes can under certain conditions behave like DNAzymes, a kind of nucleic acid enzymes with a great potential in the field of biocatalysis [7,8]. Moreover, a few DNA G-quadruplexes combined with hemin are able to effectively catalyze H_2O_2-mediated oxidation [1,2], thereby mimicking horseradish peroxidase. As an indicator of the reaction 2,2'-azino-bis(3-ethylbenzothiazoline-6-sulfonic acid)diammonium salt (ABTS) is commonly used. The oxidized $ABTS^{\bullet+}$ reaction product has a green color and can be detected spectrophotometrically [9].

DNA-metal base pairs are currently investigated because of their potential in sensing applications [10]. Some metal ions can selectively bind to a DNA bases in DNA duplexes to form metal mediated base pairs [11]. Hg^{2+} was found to interact specifically with the thymine-thymine (T-T) mismatch in the DNA duplexes [12] and similarly cytosine-cytosine (C-C) pairs are able to capture specifically Ag^+ [13]. Based on this feature, Zhou et al. constructed G-quadruplex-hemin amplified DNAzymes Ag^+ sensor based on the ability of Ag^+ to stabilize cytosine-cytosine (C–C) mismatches by forming C–Ag^+–C base pairs [14]. In the absence of Ag^+, the oligonucleotide strand forms an intramolecular duplex, which partly impairs DNAzyme activity. After the addition of Ag^+, the full DNAzyme activity is restored.

The opposite role of Ag^+ ions as an inhibitor of G-quadruplex formation was described by Zhou et al. in another paper [13]. The approach presented in that paper was based on the destruction of G-quadruplex structures by Ag^+ ions. Due to the fact that Ag^+ chelates guanine bases at the binding sites that are involved in the G-quadruplex formation [15-17], the presence of Ag^+ ions may disrupt G-quadruplex and inhibit its peroxidase activity. Besides Ag^+ ions, there are other metals and metal-based compounds, which can be detected by this assay. The ability to destroy the G-quadruplex by cisplatin was described by Wang et al. [18]. Cisplatin [*cis*-diammine-dichloroplatinum(II)] is commonly used as an anticancer drug, which binds covalently to DNA and forms several kinds of adducts [19]. It can coordinate to N7 of two neighboring guanine and/or adenine bases, as this nitrogen does not form H bonds with other bases, in the same or in opposite DNA strands.

Our aim was to investigate the effect of different reaction conditions for the formation of G-quadruplex by both spectrophotometric and electrochemical methods. It is interesting that electrochemical research on DNA is really extended and the redox behavior and adsorption processes in case of nucleic acids have been extensively studied over recent decades [20] but the redox behavior of G-quadruplex structures stared to be investigated only very recently. Electrochemical behavior of G-quadruplexes was associated by solid carbon or gold electrodes [20] and with various thrombin aptasensors based on G-quadruplex formation due to presence of guanine rich sequences [21]. In this

study, we investigated the G-quadruplex behavior in combination with other compounds on a hanging mercury drop electrode. Further, we investigated the effect of different concentrations of Ag^+ ions as an enhancer of G-quadruplex formation and cisplatin as an inhibitor of G-quadruplex formation. We also explored the ability of G-quadruplex coupling with gold magnetic nanoparticles, because the gold surface of particles allow to attach thiol modified DNA sequence via covalent thiol-gold bond [22-24], and possibility of automation of spectrophotometric assay.

2. MATERIAL AND METHODS

2.1 Chemicals

Control oligonucleotide sequence (ODN) 5´-TTA TTG CTA AGC CAA ACC C-3´, G-quadruplex forming sequence (ODNGQ1) 5´-GGG TAC GCT CTT CAA AAG AGA CCC T AC CCA AAG GGT AGG GCG GGT TGG G A-3´ described by Zhou et al. [14], G-quadruplex forming sequence with complementary chain to thiolated oligonucleotide (ODNGQ2) 5´- GTC GTC ACA CAA CAC ACT GCA GGG TAC GCT CTT CAA AAG AAG ACC CTA CCC AAA GGG TAG GGC GGG TTG GGA-3´ and thiolated complementary sequence to G-quadruplex forming oligonucleotide 5´-CTG CAG TGT GT-SH 3´, ACS water, Trizma base, potassium acetate, Triton X-100, hemin, H_2O_2, 2,2'-azinobis(3-ethylbenzothiazoline-6-sulfonic acid)diammonium salt (ABTS), silver nitrate and cisplatin and other chemicals were purchased from Sigma-Aldrich (USA) in ACS purity unless noted otherwise.

2.2 Synthesis of gold magnetic particles (AuMNPs)

The AuMNPs were prepared according to the following procedure. Two different solutions were prepared separately. *First solution*. 1.5 g of $Fe(NO_3)_3 \bullet 9H_2O$ was dissolved in 80 mL of water in a 250 mL beaker. *Second solution*. 1.4 mL of 25% NH_3 solution (*w*/*w*) was mixed with 8.6 mL of water in a screw capped tube and poured in a separate beaker. 0.2 g of $NaBH_4$ was mixed with the second solution. A magnetic stirrer was used to mix them properly. After 10 min of the mixing, the second solution was added to the first solution. The color of the solution became black with an initial frothing. Then, it was heated at 100 °C for 2 h. Further, the mixture was stirred overnight. Next day, the magnetic particles were separated from the solution by an external magnet and washed several times with water. The nanoparticles prepared from 1.5 g $Fe(NO_3)_3 \bullet 9H_2O$ as a source of iron were suspended in 80 mL of water and polyvinylpyrrolidone (10 k, 1.5 g in 20 mL of water) was added under stirring. After 3 h of stirring a solution of $HAuCl_4$ (25 mL, 1 mM) was added. The mixture was stirred for 1 h and a solution of trisodium citrate dihydrate (0.75 mL, 0.265 g/10 mL) was added. After stirring overnight, gold magnetic particles were separated by magnet, washed with water and dried at 40 ºC. Finally, the magnetic gold nanoparticles were air dried and stored in a glass container.

2.3 G-quadruplex formation

The ODN solutions (0.3 μM, final concentration) were prepared in 10 mM Tris-acetic acid (Tris-HAc) buffer (pH 7.0) containing 5 mM potassium acetate and 0.002% (*v*/*v*) Triton X-100. In the case of investigation of Ag^+ ions or cisplatin effect, different amounts of aqueous solutions of $AgNO_3$ (40 nM to 5 μM in a final volume) or cisplatin (40 nM to 3 μM in a final volume) were added in order to obtain various concentration combinations. The mixture was incubated at 25 ºC for 20 min., 3 μL of hemin (3 μM) was added and the mixture was left at 25 ºC for 1 h. For G-quadruplex colorimetric analysis, the hydrogen peroxide assay with ABTS as a chromogenic substrate was employed. Briefly to this assay, to 158 μL of sample solution, 20 μL ABTS (30 mM) and 22 μL H_2O_2 (20 mM) were added.

2.4 Isolation of nucleic acid fragment using AuMNPs

For isolation of nucleic acid fragment, 0.5, 1, 2, 3.5 and 5 mg/mL AuMNPs were used. The hybridization solution was as it follows: 0.1 M Na_2HPO_4; 0.1 M NaH_2PO_4; 0.6 M guanidinium thiocyanate (Amresco, Solon, OH, USA); 0.15 M Tris-HCl (pH 7.5) and 0.2 M NaCl. For the first hybridization, 10 μL of AuMNPs were pipetted to an Eppendorf tube within the magnetic field and washed three times with 100 μL of Tris-HAc buffer (pH 7). Afterwards, 10 μL of 100 μM ODN 5´-CTG CAG TGT GT-SH 3´ and 10 μL of Tris-HAc buffer (pH 7) was added and incubated (30 min, 25 °C) using a Multi RS-60 (Biosan Ltd., Riga, Latvia). The sample was washed 3 times with 100 μL of Tris-HAc buffer using a magnet. Subsequently, 10 μL of 100 μM G-quadruplex forming ODN sequence 5´- ATT ATT GGT AAC CTA CAC ACT GCA GGG TAC GCT CTT CAA AAG AAG ACC CTA CCC AAA GGG TAG GGC GGG TTG GGA-3´ and 10 μL of hybridization buffer was added and incubated (30 min, 25 °C) using the Multi RS-60 (Biosan Ltd., Riga, Latvia). The sample was washed 3 times with 100 μL of Tris-HAc using the magnet and diluted with ACS water to volume of 44 μL. Then, 5 μL of cut buffer (New England Biolabs, Ipswich, Great Britain) and 1 μL of restriction endonuclease PstI-HF (New England Biolabs) were added to the mixture. Then, the sample was incubated for 2 h at 37 °C and subsequently for 20 min at 80 °C using thermomixer (Eppendorf, Hamburk, Germany).

2.5 Spectrophotometric analysis

The absorption spectra of the reaction product $ABTS^{\bullet+}$ were obtained within the range from 400 to 500 nm using quartz cuvettes (1 cm, Hellma, Essex, UK) on a spectrophotometer SPECORD 210 (Analytik Jena, Jena, Germany) at 25 °C (Julabo, Labortechnik, Wasserburg, Germany). The absorbance at 422 nm was used for quantitative analysis. The changes in absorbance spectra were recorded and evaluated using the program WinASPECT version 2.2.7.0

2.6 Automated spectrophotometric analysis of G-quadruplex

For determination of G-quadruplex, a BS-400 automated spectrophotometer (Mindray, China) was used. It was composed of a cuvette space tempered to 37±1 °C, a reagent space with a carousel for reagents (tempered to 4±1 °C), a sample space with a carousel for preparation of samples, and an optical detector. Transfer of the samples and reagents was provided by robotic arm equipped with a dosing needle (error of dosage up to 5 % of volume). Cuvette contents were mixed by an automatic mixer including a stirrer immediately after addition of reagents or samples. Contamination was reduced due to its rinsing system, including rinsing of the dosing needle as well as the stirrer by MilliQ water. To the assay, 150 μL volume of reagent 1 (3.9 mM $ABTS^{\bullet+}$) and 40 μL of reagent 2 (10 mM H_2O_2) was incubated with 10 μL of sample. Absorbance was measured at $\lambda = 412$ nm after 5 minutes.

2.7 Determination of ODN – CA and G peak

Determination of ODN by square wave voltammetry was performed by 663 VA Stand (Metrohm, Switzerland) connected with AUTOLAB Analyzer (Metrohm, Switzerland) using adsorptive transfer technique and a standard cell with three electrodes arrangement. A hanging mercury drop electrode (HMDE) with a drop area of 0.4 mm^2 was used as the working electrode, Ag/AgCl/3M KCl electrode as the reference and platinum electrode as auxiliary one. For data processing GPES 4.9 software provided by Metrohm was employed. The test solutions were deoxygenated prior to measurements by purging with argon (99.999%). For the CA peak analysis, the Tris buffer (10 mM Trizma base adjusted to pH = 5 by 1 M acetic acid) was used as a supporting electrolyte. The parameters of the measurement were as follows: initial potential 0 V, end potential -1.7 V, deoxygenating with argon 30 s, accumulation time 120 s, step potential 5 mV, modulation amplitude 25 mV, volume of injected sample: 5 μl, and volume of measurement cell 2 mL (5 μL of sample and 1995 μL supporting buffer). For the G peak analysis, the 50 mM sodium phosphate with 0.3 M ammonium formate (pH 6.9) was used as a supporting electrolyte and the parameters of the measurement were as follows: initial potential -0.1 V, first vertex potential -1.75 V, second vertex potential -0.1 V, voltage step 5 mV, sweep rate 1 V/s, deposition potential -0.1 V, deposition time 120 s, initial purge time 120 s, equilibration time 5 s. Volume of injected sample: 10 μL, volume of measurement cell 1 mL (10 μL of sample and 990 μL of supporting electrolyte).

2.8 Determination of platinum by atomic absorption spectrometry

Platinum was determined on 280Z Agilent Technologies atomic absorption spectrometer (Agilent, USA) with electrothermal atomization and Zeeman background correction. Platinum ultrasensitive hollow cathode lamp (Agilent) was used as the radiation source (lamp current 10 mA). The spectrometer was operated at 265.9 nm resonance line with spectral bandwidth of 0.2 nm. The samples prepared as described above were purified using Amicon Cut-off filters (Amicon Ultra-0.3 K Centrifugal Filter, Merck Millipore, Germany). Both, eluate and retentate were analyzed by AAS.

2.9 Descriptive statistics

Data were processed using MICROSOFT EXCEL® (USA). Results are expressed as a mean value ± standard deviation (S.D.) unless noted otherwise (EXCEL®). The detection limits (3 signal/noise, S/N) were calculated according to Long and Winefordner [25], whereas N was expressed as standard deviation of noise determined in the signal domain unless stated otherwise.

3. RESULTS AND DISCUSSION

3.1 The characterization of G-quadruplex

In the first part of the work, the G-quadruplex forming sequence (ODNGQ1) was characterized spectrophotometrically. The scheme of G-quadruplex formation is shown in Fig. 1A. The ODNGQ1 consists of two domains that form a duplex in the presence of Tris buffer. The first domain (black one in Fig. 1A I) contains two cytosine-cytosine (C-C) mismatched sequences, which stabilize the intramolecular duplex. The second domain (purple one in Fig. 1A I) of the guanine rich part of the ODN sequence has an ability to form G-quadruplex with the catalytic activity in the presence of K^+ ions (Fig. 1A II). When hemin is added [14], this structure has the DNAzyme activity and catalyzes the H_2O_2-mediated oxidation of ABTS producing the free-radical cation ABTS$\bullet^+$ (Fig. 1A III) showing the maximal absorbance at 422 nm [14]. The change of this photometric signal allows us to monitor formation of the G-quadruplex. The mentioned ODN sequence has the ability to bind Ag^+ ions in the cytosine rich domain while the Ag^+ stabilizes the C-C mismatches by forming C-Ag^+-C base pairs [14]. This phenomenon increases peroxidase activity of the G-quadruplex complex with hemin (Fig. 1A IV).

Subsequently, we compared the G-quadruplex forming capability of ODN sequence, which is not allowed to form G-quadruplex, ODN sequence forming G-quadruplex (ODNGQ1) and ODN sequence forming G-quadruplex with complementary sequence to AuMNPs probe (ODNGQ2). Each ODN (0.3 μM) was prepared according to section "*G-quadruplex formation"* and spectrophotometric signal was detected. Depending on the signal change, we observed the DNAzyme activity mediated by H_2O_2 catalyzed reaction of ABTS to ABTS$\bullet^+$. It clearly follows from the results obtained that the ODN sequence lacking guanines does not show DNAzyme activity, whereas the sequence capable of forming G-quadruplex structure (ODNGQ1) containing guanines exhibited higher spectrophotometric signal at 422 nm, which indicated G-quadruplex formation (Fig. 1B). In comparison of both guanine rich ODN sequences (ODNGQ1 and ODNGQ2), the higher spectrophotometric signal (0.40 ±0.01 AU, was observed for shorter sequence (ODNGQ1 - data not shown). The whole spectra within the wavelengths from 400 to 500 nm are shown in Fig. 1B. The ODNGQ1 (0.3 μM) provided no signal in Tris buffer, ODNGQ1 exhibited a small signal (4 % maxima) in a presence of K^+ ions, which increased after the hemin addition. The highest signal was reached after the addition of Ag^+ ions (40 nM) to the mixture of ODNGQ1, K^+ ions and hemin.

Further, the electrochemical analysis was performed. It is commonly known that nucleic acids provide two electrochemical signals: i) the reductive signal of adenine and cytosine moieties (CA peak) at the potential of -1.4 V, and ii) the oxidative signal of guanine moiety (G peak) at of potential -0.25 V [26]. Therefore, we aimed our attention at these peaks and found the different results by the electrochemical measurement of CA peak and G peak (Figs. 1C and 1D). The highest CA peak was found at pure ODNGQ1 in Tris buffer. The addition of K^+ ions caused a decrease in the electrochemical signal, which indicated the formation of the G-quadruplex. Further, a small decrease of the CA peak was observed after addition of hemin. No change in the CA peak was observed after addition of 40 nM Ag^+ ions (Fig. 1C). In the case of G peak, it was not possible to detect signal of ODNGQ1 alone without K^+ ions. The highest signal was obtained in case of the mixture of ODNGQ1 and K^+ ions. After addition of hemin to this mixture, the G peak disappeared and further addition of Ag^+ ions had no influence on the height of the G peak (Fig. 1D).

3.2 An influence of concentrations of Ag^+ ions on DNAzyme activity

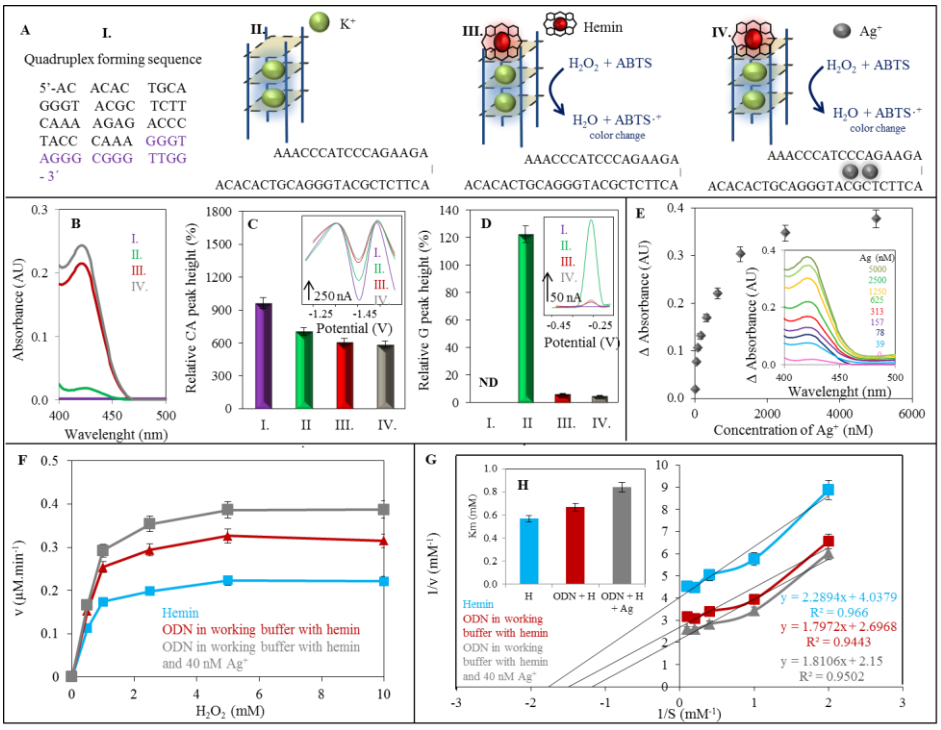

Figure 1. (**A**) Scheme of the ODNGQ1 forming G-quadruplex. Formation of the G-quadruplex from (I) ODNGQ1 rich in guanines; (II) in the presence of K^+ ions; (III) K^+ ions and hemin; and/or (IV) K^+ ions, hemin and Ag^+ ions. (**B**) Spectrophotometric detection of peroxidase activity of G-quadruplex with ABTS oxidation by H_2O_2; (**C**) The electrochemical signal of CA peak, and (**D**) the electrochemical signal of G peak of 0.3 μM ODN rich in guanines obtained in (I) 10 mM Tris buffer (pH 7); (II) in 5 mM K^+ ions; (III) in 5 mM K^+ ions with hemin; and/or (IV) in 5 mM K^+ ions with hemin and 40 nM Ag^+ ions. (**E**) Dependence of differential absorbance measured at 422 nm on the concentration of Ag^+ ions within the range from 40 to 5000 nM. (**F**) Michaelis-Menten and (**G**) Lineweaver-Burk plots using various concentrations of H_2O_2 as a substrate (0.62; 1.25; 2,5; 5; 10 and 20 mM). (**H**) K_M of the analyzed solutions. The results are expressed as means value ± standard deviations from 3 measurements.

An effect of Ag^+ ions concentrations (40 nM – 5000 nM) was examined spectrophotometrically as well. As the formation of G-quadruplex is possible only in the presence of K^+ ions, all analyses were performed in Tris acetate buffer of pH 7.0 and 5 mM concentrations of K^+ ions. The results are shown in Fig. 1E. It clearly follows from them that the increasing concentration of Ag^+ ions caused an increase in catalytic activity of DNAzyme expressed as a growing trend of the absorbance.

3.3 Enzyme kinetics of peroxidase activity of G-quadruplex-hemin DNAzyme

In the following experiments, the enzymatic activity of G-quadruplex-hemin DNAzyme was tested (Fig. 1F). The kinetic study was performed according to the Michaelis–Menten theory, which allows analyzing quantitatively the enzymatic kinetics. Michaelis–Menten constant (K_M), maximum velocity at which the enzyme catalyzed a reaction (V_{max}), catalytic constant (K_{cat}) and substrate specifity (K_{cat}/K_m) were obtained experimentally using the Lineweaver-Burk equation within the H_2O_2 concentration range from 0.5 to 10 mM (Fig. 1G). In spite of the fact that 0.3 μM hemin showed the strongest affinity to substrate (K_m 0.57 mM) comparing to 0.3 μM G-quadruplex (K_m 0.67 mM) and the complex of 0.3 μM G-quadruplex with 40 nM Ag^+ ions (K_m 0.84 mM), the highest velocity of enzymatic reaction (V_{max}) was achieved by the G-quadruplex-Ag^+ complex as 0.47 $mM.min^{-1}$. The decrease of velocity was estimated as V_{max} 0.37 $mM.min^{-1}$ in the case of quadruplex and V_{max} 0.25 $mM.min^{-1}$ in the case of hemin. The expression of the enzyme activity using catalytic constant (K_{cat}) showed that the enzymatic activity of hemin (830 min^{-1}) is the lowest of studied samples. In the case of quadruplex, K_{cat} is 1240 min^{-1} and for the G-quadruplex-Ag^+ complex 1550 min^{-1}. The calculated substrate specificity (K_{cat}/K_M) had the strongest specifity for G-quadruplex and G-quadruplex-Ag^+ complex (1850 and 1840 $mM^{-1}\cdot min^{-1}$, respectively) when compared to hemin alone (1460 $mM^{-1}\cdot min^{-1}$).

3.4 Influence of various ions on G-quadruplex formation revealed by spectrophotometric methods

It has been observed that the G-quadruplex formation required the presence of monovalent cations such as K^+, Na^+, NH_4^+, Cs^+, and/or Li^+ [6]. In our experiment, we studied spectrophotometrically the G-quadruplex formation with K^+, Na^+ and NH_4^+ ions. The samples were prepared in the Tris acetate buffer (pH 7) with concentration of K^+, Na^+ or NH_4^+ ions within the range from 1 to 20 mM. The whole spectra obtained for K^+, Na^+ or NH_4^+ additions within the wavelength range from 400 to 500 nm are shown in Figs. 2A, 2B and 2C, respectively. Diagrams of the dependence of relative absorbance (%) recorded at 422 nm on the increasing concentration of K^+, Na^+ or NH_4^+ ions are shown in Figs. 2D, 2E and 2F, respectively. In the agreement with a widely known fact that K^+ ions are the most suitable for the stabilization of the G-quadruplex structure in comparison with Na^+ or NH_4^+ ions [6], our results confirmed that the K^+ ion has the strongest influence on the formation of G-quadruplex and on the increase of peroxidase activity in the presence of hemin. The highest observed absorbance was 1.2 AU, which was measured in the presence of 20 mM of K^+ ions.

Fig. 2D shows the dependence of G-quadruplex formation on the concentration of K^+ ions. The 15% ±5% increase of spectrophotometric signal is obvious from 1 mM to 20 mM K^+ ions.

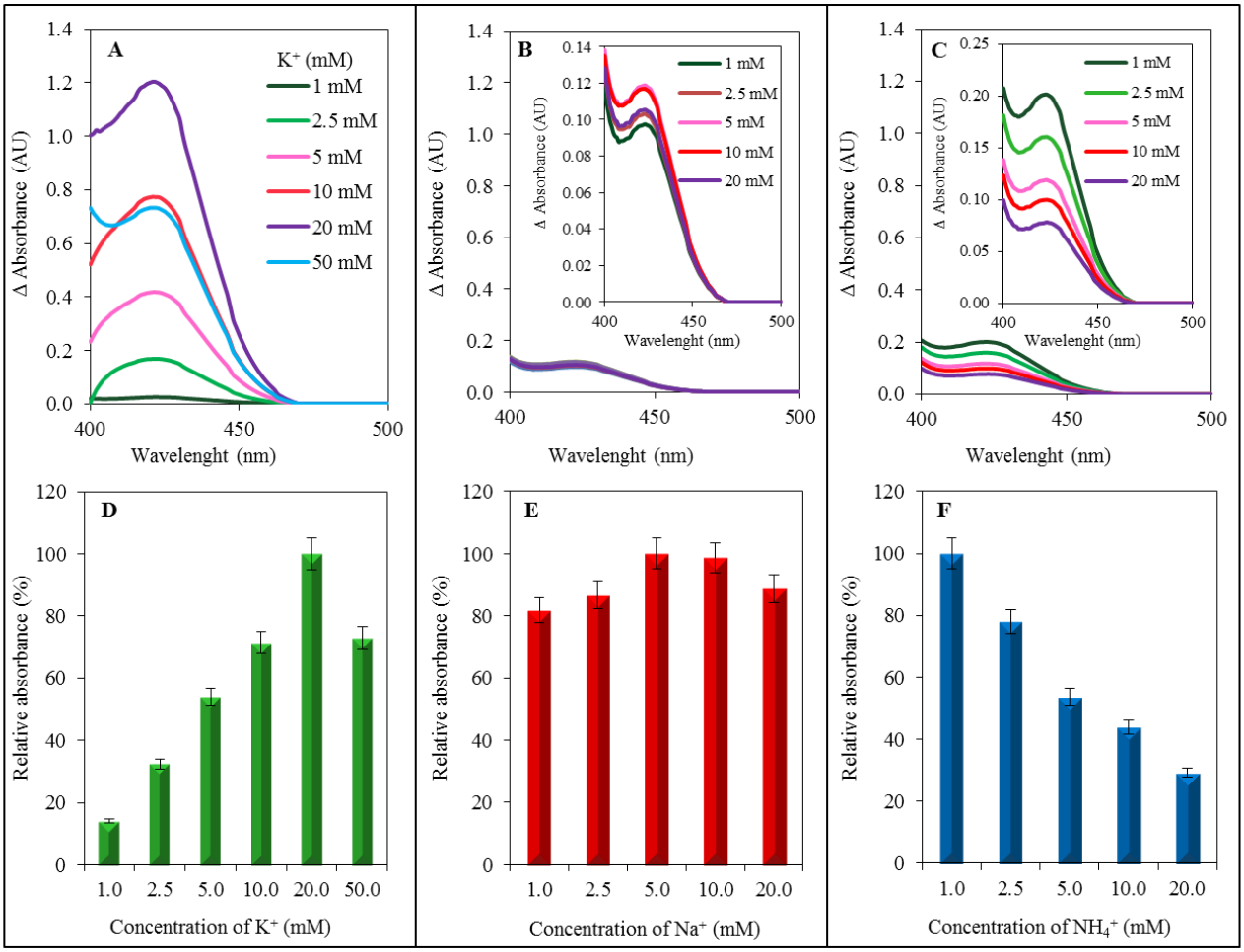

Figure 2. The dependence of G-quadruplex formation of ODNGQ1 on the increasing concentration of cations: (**A**) K^+, (**B**) Na^+ and (**C**) NH_4^+. Dependence of relative absorbance (%) recorded at 422 nm on the increasing concentration of cations as (**D**) K^+, (**E**) Na^+ and (**F**) NH_4^+ ions. The highest absorbance of G-quadruplex formed in the presence of each type of ions is expressed as 100 %. The results are expressed as means value ± standard deviations from 3 measurements.

In contrary to K^+, Na^+ ions in the concentration range 1 – 20 mM exhibited lower effect on the G-quadruplex formation. Fig. 2E shows that 1 - 5 mM Na^+ ions, caused only 20% ±5% increase in absorbance while 10 and 20 mM of Na^+ ions leaded to absorbance decreasing by 20% ±5 %. The lower influence of Na^+ ions on the G-quadruplex formation in comparison to K^+ ions clearly follows. The opposite trend was observed in the case of NH_4^+ ions, where the lowest concentration of NH_4^+ ions (1 mM) had the strongest effect on the G-quadruplex formation (Fig. 2F) and the higher concentration of NH_4^+ ions (10 and 20 mM) caused the 80% ±5% decrease in absorbance.

3.5 Disruption of the G-quadruplex with cisplatin (CisPt)

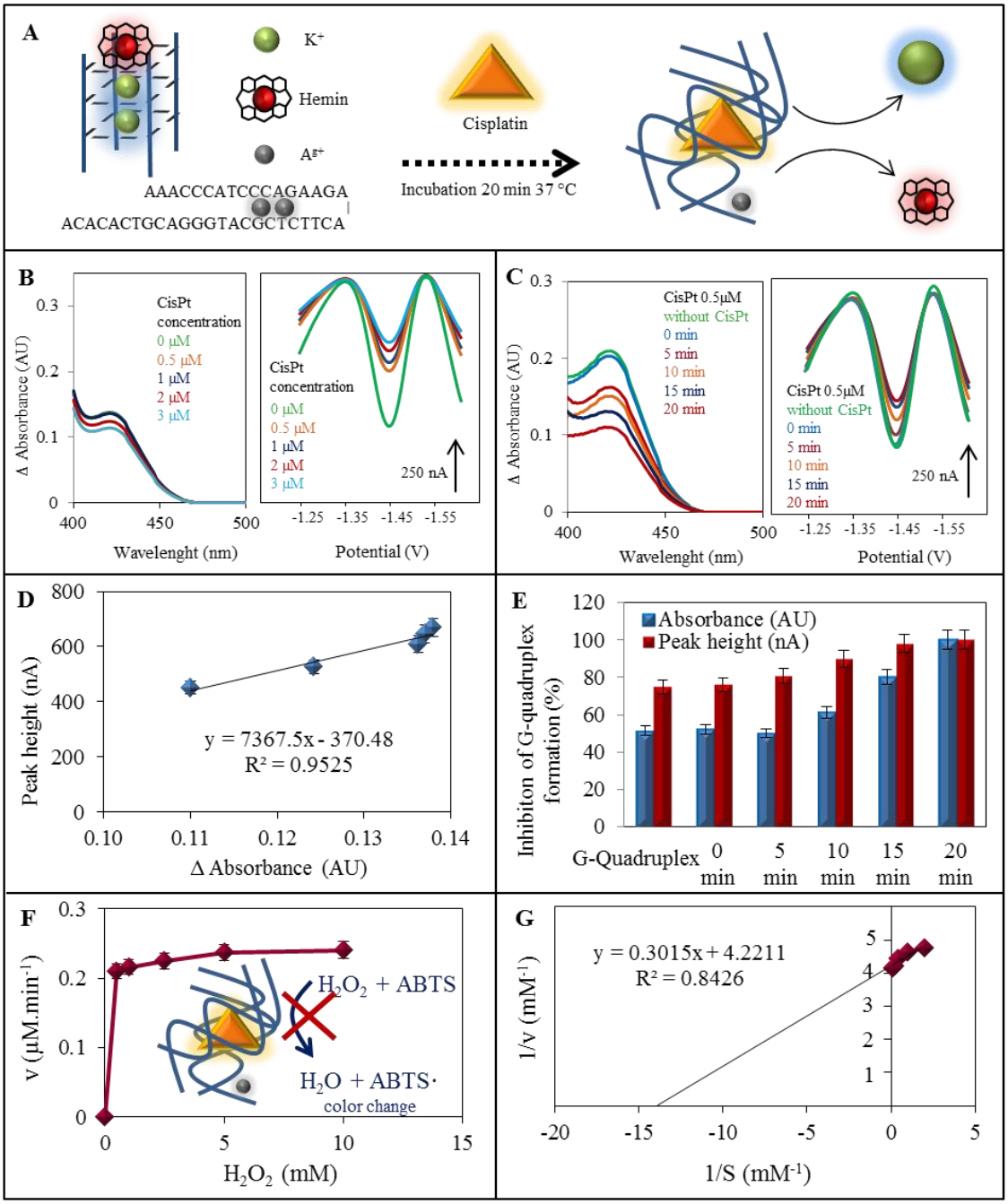

Figure 3. (**A**) Scheme of G-quadruplex interaction with cisplatin (CisPt). (**B**) Spectral (left) and electrochemical signal (right) of inhibition of G-quadruplex formation by CisPt. (**C**) Differential absorbance (left) and electrochemical signal (right) of time-dependent measurement of inhibition of G-quadruplex formation caused by addition of 0.5 µM CisPt. (**D**) Time dependence of inhibition of the G-quadruplex formation caused by 0.5 µM CisPt. The results are expressed as a percentage where 100% is the strongest inhibition of G-quadruplex formation obtained after 20 minutes of interaction. (**E**) Correlation of spectrophotometric and electrochemical data of inhibition of the G-quadruplex formation by 0.5 - 3 µM of CisPt. The results are expressed as means value ± standard deviations from 3 measurements. (**F**) Michaelis-Menten and (**G**) Lineweaver-Burk plots using different concentrations of H_2O_2 as the substrate (0.62; 1.25; 2,5; 5; 10 and 20 mM).

Table 1. Comparison of Michaelis–Menten constant (K_M), maximum velocity, at which the enzyme catalyzed a reaction (V_{max}), catalytic constant (K_{cat}) and substrate specifity (K_{cat}/K_m) for 0.3 μM hemin, 0.3 μM G-quadruplex, 0.3 μM G-quadruplex with 40 nM Ag^+ ions complex and 0.3 μM G-quadruplex with 2 μM CisPt complex.

Compound	K_M		V_{max}		K_{cat}		K_{cat}/K_M	
	mM		mM.min^{-1}		min^{-1}		mM^{-1}·min^{-1}	
Hemin	0.57	±0.03	0.25	±0.01	830	±40	1460	±70
G-quadruplex with hemin	0.67	±0.03	0.37	±0.02	1240	±60	1850	±90
G-quadruplex-Ag^+ complex	0.84	±0.04	0.47	±0.02	1550	±80	1840	±90
G-quadruplex-CisPt complex	0.13	±0.01	0.14	±0.01	460	±20	3430	±200

The ability of cisplatin (CisPt) to intercalate into guanine-guanine basepairs, change the G-quadruplex structure and disrupt the DNAzyme activity (schematically shown in Fig. 3A) was electrochemically detected by Wang et al. [18]. We utilized this finding for studying the interaction of CisPt with G-quadruplex using spectrophotometry assay and electrochemical measurement employing the HMDE. Firstly, we used different concentration of CisPt (0.5 – 3 μM) and studied its effect after 20 minutes of application. Even the lowest concentration of CisPt caused a dramatic decrease in the cathodic CA peak (Fig. 3B). The interaction of CisPt (0.5 – 3 μM) after 20 min incubation was also confirmed using atomic absorption spectrometry showing that higher applied concentration of CisPt caused the corresponding increase of intercalated platinum concentration (data not shown).

The time-dependent measurement of the inhibition of the G-quadruplex formation caused by 0.5 μM CisPt was also investigated. The reaction was monitored spectrophotometrically and electrochemically every 5 minutes and the results were compared to control signal of G-quadruplex (Fig. 3C). The spectrophotometric results showed a gradual decrease in the DNAzyme activity with the strongest effect in the twentieth minute compared to control G-quadruplex. These results confirm that cisplatin changes the G-quadruplex structure and also interferes with the DNAzyme activity. The CA peak decreased with the increasing time of interaction (Fig. 3C). This decrease is probably caused by CisPt binding between guanine and adenine as it was described recently [27]. A correlation of spectrophotometric and electrochemical results is evident with the coefficient of determination $R^2 = 0.9525$ (Figs. 3D and 3E). The enzymatic activity of 0.3 μM G-quadruplex and 2 μM CisPt complex was also described by Michaelis-Menten model (Fig. 3F) and Lineweaver-Burk equation (Fig. 3G) within H_2O_2 concentration range from 0.5 to 10 mM. The G-quadruplex-CisPt complex exhibited greater substrate affinity for 85% (K_M 0.13 mM) in comparison with the G-quadruplex-Ag^+ complex while the maximal velocity of enzymatic reaction (V_{max} 0.14 mM.min^{-1}) was by 70% lower than that of G-quadruplex-Ag^+. Expression of the enzyme activity (K_{cat}) leaded to the lowest overall catalytic constant (K_{cat} 460 min^{-1}). Substrate specifity (K_{cat}/K_M) was estimated as 3430 mM^{-1}·min^{-1} (Tab. 1). These results correspond with higher substrate affinity of the G-quadruplex-CisPt complex.

3.6 Identification of nucleic acid fragment

Magnetic nanoparticles are widely used for DNA isolation from various samples [28-31]. Modification of their surface could provide the specific interaction with appropriate nucleic acid sequence [32].

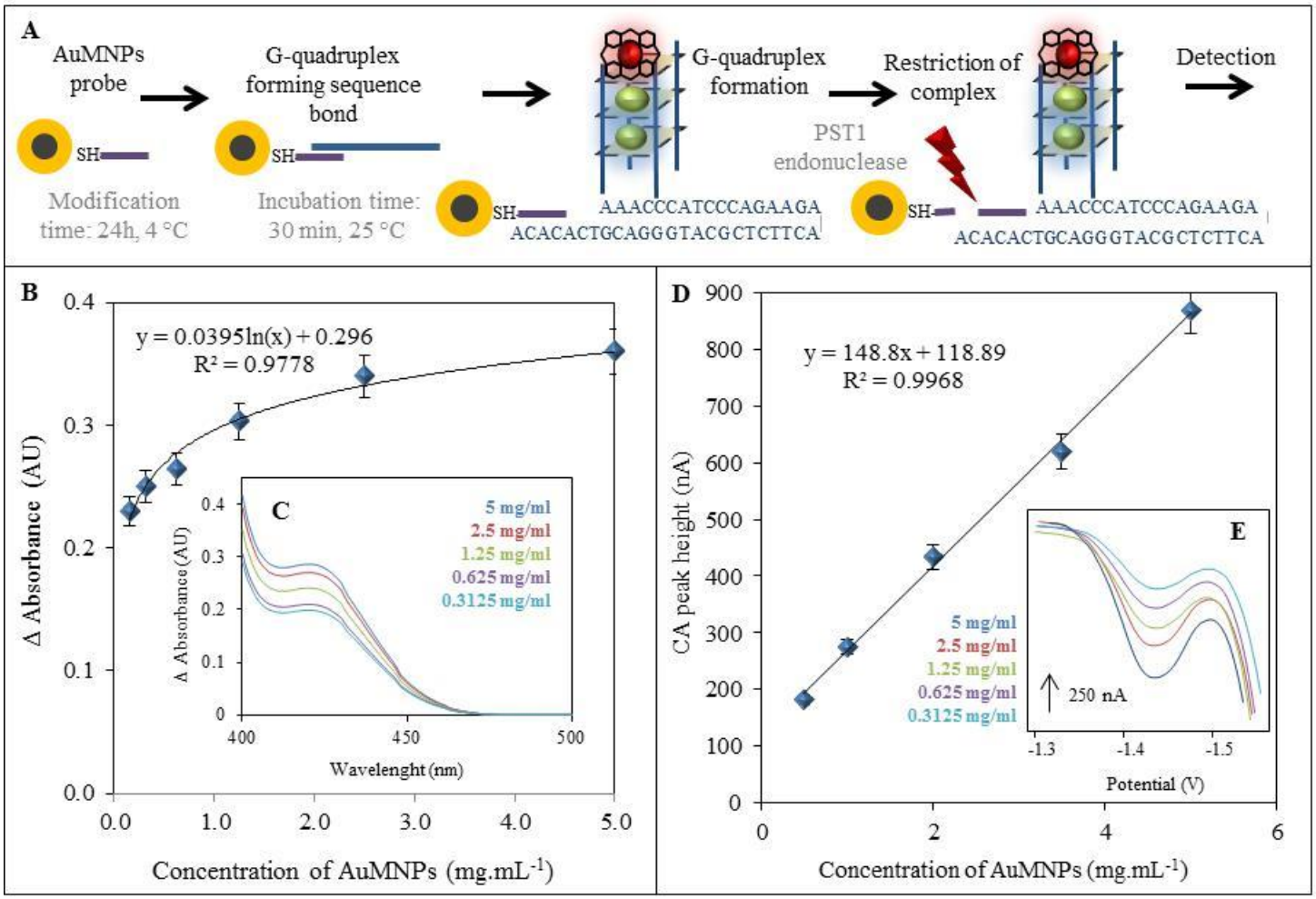

Figure 4. (**A**) Experimental scheme of thiolated oligonucleotide isolation using AuMNPs followed by the G-quadruplex formation for spectrophotometric and electrochemical detection. (**B**) Dependence of absorbance of isolated G-quadruplex on AuMNPs (0 – 10 mg/mL) concentration measured in ABTS-H_2O_2 system; 3 mM ABTS and 2 mM H_2O_2 were used for detection at 422 nm. (**C**) Differential absorbance spectra of G-quadruplex at various concentrations of AuMNPs (0.2 – 10 mg/mL). (**D**) Dependence of AuMNPs (0.5 – 10 mg/mL) concentration on electrochemical signal of G-quadruplex. (**E**) Cyclic voltammograms of CA of isolated G-quadruplex by AuMNPs (0 – 10 mg/mL) of various concentrations.

In our study we used thiolated ODN sequence, with affinity to AuMNPs and attached complementary ODN to G-quadruplex forming sequence (ODNGQ2), which allowed for spectrophotometric determination of this complex. The experimental scheme is shown in Fig. 4A. Firstly, we modified the various concentrations (0.5 – 5 mg/mL) of AuMNPs by thiolated

oligonucleotide (10 μM) and AuMNPs probe was treated 1 hour with complementary G-quadruplex forming sequence (ODNGQ2; 10 μM). To prevent any interference of AuMNPs to the spectrophotometric and electrochemical determination, the endonuclease PSTI-HF was used to cleave the particles from the formed complex and the quantity of thiolated ODN sequence corresponded with spectrophotometric and electrochemical signal of G-quadruplex. As it is shown in Figs. 4B and C, higher of applied concentration of AuMNPs increased the absorbance of G-quadruplex. We estimated the linear trend with the following equation $y = 0.0395\ln(x) + 0.296$, $R^2 = 0.9778$, RSD = 5 % and n = 3. Electrochemical analysis of G-quadruplex confirmed the spectrophotometric results and the correlation analysis showed the linear trend with the following equation $y = 148.8x + 118.89$, $R^2 = 0.9968$.

3.7 Automation of the G-quadruplex detection

Spectrophotometric determination of G-quadruplex using the ABTS assay requires the precise timing between reagent addition and detection due to rapid enzymatic kinetic. Automatic spectrophotometric analyzer allowed us precise dosing the sample and reagents, meticulous timing and elimination of human failure during pipetting. For an automated method evaluation the calibration curves of both methods were compared. The obtained data are summarized in Tab. 2. The ABTS manual assay showed the linear dynamic range 40 – 300 nM with the regression equation $y = 0.3732x + 0.0307$. Limit of detection (LOD, 3 S/N) was estimated to 10 nM and Limit of quantification (LOQ, 10 S/N) to 40 nM, respectively. For the ABTS automated assay the regression equation was determined as $y = 0.3065x - 0.0072$ within the dynamic range 100 – 500 nM. LOD 50 nM and LOQ 100 nM were calculated. The automated ABTS assay was found to be more precise and more rapid at the expense of limit of detection in the linear dynamic range. However, manual assay is still more sensitive than the automated one.

Table 2. Analytical parameters of manual and automated ABTS assay. LOD was calculated as 3 S/N and LOQ 10 S/N (n = 3).

	Regression equation	Linear dynamic range	R^2	LOD	LOQ	RSD
		nM		nM	nM	%
Manual assay	$y = 0.3732x + 0.0307$	40 - 300	0.991	10	40	5
Automated assay	$y = 0.3065x - 0.0072$	100 - 500	0.991	50	100	5

4. CONCLUSIONS

Oligodeoxynucleotides (ODNGQ1 and ODNGQ2) forming G-quadruplexes were studied. The influence of various concentrations of potassium, sodium or ammonium ions on G-quadruplex formation was investigated both spectrophotometrically (detection of oxidized ABTS product) and

electrochemically (using height of the CA and G peaks). The most appropriate conditions for the highest peroxidase activity of G-quadruplex and the maximum CA peak height were both found in the presence of potassium ions in concentration of 20 mM. Further, we studied the effect of cisplatin on G-quadruplex formation. It was found that even 0.5 μM of CisPt caused significant decrease in CA peak and the inhibition of the peroxidase activity. The gold magnetic particle utilizing formation of G-quadruplex can be further modified and therefore, its potential can be developed.

ACKNOWLEDGEMENTS
Financial support from the following project GACR P102/11/1068 is highly acknowledged. This publication was also supported by the Slovak Research and Development Agency under the contract No. APVV-0797-11. The authors wish to express their thanks to Radek Chmela for perfect sample preparation, Sona Krizkova and Renata Kensova for AAS analysis.

References

1. P. Travascio, Y. F. Li and D. Sen, *Chem. Biol*., 5 (1998) 505.
2. P. Travascio, P. K. Witting, A. G. Mauk and D. Sen, *J. Am. Chem. Soc*., 123 (2001) 1337.
3. P. Jones, D. Mantle, D. M. Davies and H. C. Kelly, *Biochemistry*, 16 (1977) 3974.
4. B. C. Saunders and B. P. Stark, *Tetrahedron*, 23 (1967) 1867.
5. J. L. Huppert, *Biochimie*, 90 (2008) 1140.
6. D. Sen and W. Gilbert, *Nature*, 344 (1990) 410.
7. R. R. Breaker, *Nat. Biotechnol*., 15 (1997) 427.
8. D. Sen and C. R. Geyer, *Curr. Opin. Chem. Biol*., 2 (1998) 680.
9. J. Sochor, L. Nejdl, B. Ruttkay-Nedecky, A. Bezdekova, K. Lukesova, O. Zitka, N. Cernei, P. Mares, M. Pohanka, V. Adam, P. Babula, M. Beklova, L. Zeman and R. Kizek, *J. Appl. Biomed*., 12 (2014) 97.
10. L. Nejdl, B. Ruttkay-Nedecky, J. Kudr, S. Krizkova, K. Smerkova, S. Dostalova, M. Vaculovicova, P. Kopel, J. Zehnalek, L. Trnkova, P. Babula, V. Adam and R. Kizek, *Int. J. Biol. Macromol.*, 64 (2014) 281.
11. G. H. Clever, C. Kaul and T. Carell, *Angew. Chem.-Int. Edit*., 46 (2007) 6226.
12. S. M. Jia, X. F. Liu, P. Li, D. M. Kong and H. X. Shen, *Biosens. Bioelectron*., 27 (2011) 148.
13. X. H. Zhou, D. M. Kong and H. X. Shen, *Anal. Chem*., 82 (2010) 789.
14. X. H. Zhou, D. M. Kong and H. X. Shen, *Anal. Chim. Acta*, 678 (2010) 124.
15. R. M. Izatt, Christen.Jj and J. H. Rytting, *Chem. Rev*., 71 (1971) 439.
16. J. V. Burda, J. Sponer and P. Hobza, *J. Phys. Chem*., 100 (1996) 7250.
17. X. X. Liu, W. Li, Q. P. Shen, Z. Nie, M. L. Guo, Y. T. Han, W. Liu and S. Z. Yao, *Talanta*, 85 (2011) 1603.
18. G. F. Wang, X. P. He, L. Chen, Y. H. Zhu, X. J. Zhang and L. Wang, *Biosens. Bioelectron*., 50 (2013) 210.
19. V. Marini, J. Kasparkova, O. Novakova, L. M. Scolaro, R. Romeo and V. Brabec, *J. Biol. Inorg. Chem*., 7 (2002) 725.
20. A.-M. Chiorcea-Paquim and A. M. Oliveira-Brett, *Electrochim. Acta*, 126 (2014) 162.
21. H. Fan, Z. Chang, R. Xing, M. Chen, Q. Wang, P. He and Y. Fang, *Electroanalysis*, 20 (2008) 2113.
22. I. Robinson, L. D. Tung, S. Maenosono, C. Waelti and N. T. K. Thanh, *Nanoscale*, 2 (2010) 2624.
23. K. A. Stevenson, G. Muralidharan, L. Maya, J. C. Wells, J. Barhen and T. Thundat, *J. Nanosci. Nanotechnol.*, 2 (2002) 397.

24. J. Kudr, L. Nejdl, S. Skalickova, B. Ruttkay-Nedecky, M. A. M. Rodrigo, S. Dostalova, A. M. J. Jinemez, D. Chudobova, K. Cihalova, M. Konecna, P. Kopel, J. Kynicky, V. Adam and R. Kizek, *Int. J. Electrochem. Sci*., 9 (2014) 3409.
25. G. L. Long and J. D. Winefordner, *Anal. Chem.*, 55 (1983) A712.
26. E. Palecek, *Nature*, 188 (1960) 656.
27. M. Crul, R. C. A. M. van Waardenburg, J. H. Beijnen and J. H. M. Schellens, *Cancer Treat. Rev*., 28 (2002) 291.
28. O. Zitka, N. Cernei, Z. Heger, M. Matousek, P. Kopel, J. Kynicky, M. Masarik, R. Kizek and V. Adam, *Electrophoresis*, 34 (2013) 2639.
29. L. Krejcova, D. Hynek, P. Kopel, V. Adam, J. Hubalek, L. Trnkova and R. Kizek, *Chromatographia*, 76 (2013) 355.
30. M. Vaculovicova, K. Smerkova, J. Sedlacek, J. Vyslouzil, J. Hubalek, R. Kizek and V. Adam, *Electrophoresis*, 34 (2013) 1548.
31. O. Zitka, S. Skalickova, M. A. M. Rodrigo, L. Krejcova, P. Kopel, V. Adam and R. Kizek, *Int. J. Electrochem. Sci.*, 8 (2013) 12628.
32. J. A. Jung, Y. B. Kim, Y. A. Kim, S. B. Ryu and V. Kim, *J. Nanopart. Res*., 13 (2011) 2361.